Synthesis and AO Resistant Properties of Novel Polyimide Fibers Containing Phenylphosphine Oxide Groups in Main Chain

Yong Zhao,（赵勇）Guomin Li,（李国民）Fangfang Liu,（刘芳芳）Xuemin Dai,（代学民） Zhixin Dong,*（董志鑫）Xuepeng Qiu*（邱雪鹏）

Polymer Composites Engineering Laboratory, Changchun Institute of Applied Chemistry, Chinese Academy of Sciences, Changchun 130022, P. R. China

（中国科学院长春应用化学研究所，高分子复合材料工程实验室）

ABSTRACT A series of co-polyimide (PI) fibers containing phenylphosphine oxide (PPO) group were synthesized by incorporating the bis(4-aminophenoxy) phenyl phosphine oxide (DAPOPPO) monomer into the PI molecular chain followed by dry-jet wet spinning. The effects of DAPOPPO molar content on the AO resistance of the fibers were investigated systematically. When the AO fluence increased from 0 to 3.2×10^{20} atoms cm^{-2}, the mass loss of the fibers showed dependence on DAPOPPO molar content in co-PI fibers. PI fiber containing 40% DAPOPPO showed lower mass loss comparing to those containing 0% and 20% DAPOPPO. At higher AO fluence, higher DAPOPPO content gave rise to dense carpet-like surface of fibers. XPS results indicated the passivated phosphate layer deposited on the fiber surface when exposed to AO, which effectively prevented fiber from AO erosion. With the DAPOPPO content increasing from 0% to 40%, the retentions of tensile strength and initial modulus for the fibers exhibited clear growth from 44% to 68% and 59% to 70% after AO exposure with the fluence of 3.2×10^{20} atoms cm^{-2}. The excellent AO resistance benefits the fibers to apply in low Earth orbit as flexible construction components.

KEYWORDS Polyimide fibers; Bis(4-aminophenoxy) phenyl phosphine oxide (DAPOPPO); Dry-jet wet spinning; AO resistance

1. INTRODUCTION

Atomic oxygen (AO) attack to polymer materials on the surface of spacecraft in low Earth orbit (LEO, 200-700 km) is a serious problem for threatening spacecraft in-orbit safe operation and service life[1-3]. As one of critical materials, polyimide (PI) fibers and their fabrics generally were used to flexible construction components of spacecraft installed on the external surfaces, including different fastener assemblies, tensional cables, flexible sheetings and screens, railings, and safety lines[4-8]. When suffered AO attack, surface destroy, mass loss and degradation of the mechanical properties for the fibers happened[9-11].

Generally, polymer materials are typically protected by the deposition of a coating, often aluminum oxide, silicon dioxide, tin oxide, or indium tin oxide based, which could resist to degradation of AO. However, there are restrictions on the shape and size of polymer materials that can be coating protected. Meanwhile, the thermal expansion coefficients of these inorganic coatings show significant difference from those of polymers, leading to cracks developing during thermal cycling. Moreover, folding or bending with small radii cannot be allowed.[2, 12-15]. Consequently, alternative and self-regenerative methods of protection are adopted. The strategy of incorporation phenylphosphine oxide (PPO) groups into polymer chain has been focused on improving the AO resistance. Connell and co-workers at NASA Langley have developed a series of PPO containing aromatic polymers, which provides AO and oxygen plasma resistance[16-20]. It had been demonstrated that the polymers typically contained 3–7% by weight of phosphorous exhibited high glass transition temperatures and Young's moduli. Based on those, series of PI containing PPO groups have been prepared, which exhibit excellent AO resistance, adhesion properties to metal substrates and miscibility with many thermoplastic and thermosetting polymers [10, 14, 21-27].

* Correspondence to: Xuepeng Qiu E-mail: xp_q@ciac.ac.cn

* Correspondence to: Zhixin Dong E-mail: zxdong@ciac.ac.cn

Therefore, aiming to fabricate PI fibers containing PPO groups to use in space, bis(4-aminophenoxy) phenyl phosphine oxide (DAPOPPO) was designed and synthesized. Subsequently, series of co-PI fibers were prepared by polycondensation of the above diamine monomer with commercially available aromatic dianhydride and diamine, followed by dry-jet wet spinning. The AO resistance, morphology, thermal and mechanical properties of the co-PI fibers were investigated systemically.

2. EXPERIMENTAL SECTION

Chemicals and Materials

Phenyl phosphoric dichloride (PPDC) (TCI Company, China), *p*-nitrophenol (TCI Company, China), and N,N'-Dicyclohexylcarbodie (TCI Company, China) were used as received. 1,8-Diazabicyclo [5.4.0] undec-7-ene (DBU), 4,4′-oxydianiline (4,4′-ODA) and pyromellitic dianhydride (PMDA) were purchased from Shanghai Research Institute of Synthetic Resins. PMDA was dried in vacuum at 260 °C overnight prior to use. Triphenylphosphine, dichloromethane (CH_2Cl_2), petroleum ether, ethyl acetate and N,N′-dimethyacetamide (DMAc) were purchased from Shanghai Darui Fine Chemical Co., Ltd. and used without further purification.

Monomers synthesis

The monomer, bis(4-aminophenoxy) phenyl phosphine oxide (DAPOPPO), was synthesized according to the previous reports[28, 29] with some modification and the synthesis route was shown in **SCHEME 1**. The details are as follows:

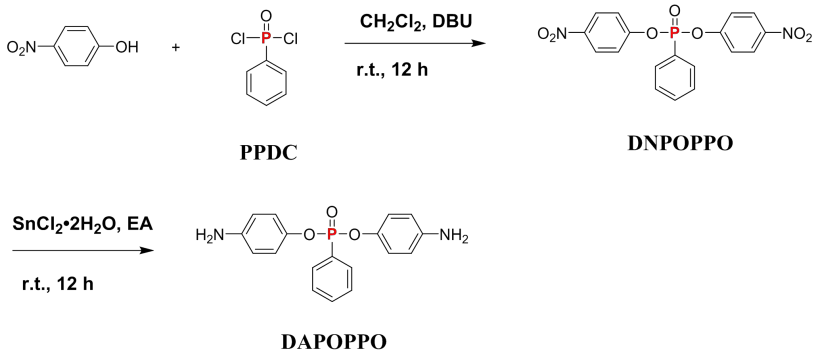

SCHEME 1. Synthesis route of phosphorous-containing diamine DAPOPPO.

Synthesis of bis(4-nitrophenoxy) phenyl phosphine oxide (DNPOPPO)
p-Nitrophenol (389.51 g, 2.8 mol) was stirred with 8000 mL of CH_2Cl_2 in a round-bottom flask. Distilled dry DBU (425.97 g, 2.8 mol) was added into the solution and then the solution was cooled to 0 °C in an ice bath. After adding DMAc (20 g), a solution of PPDC (288.58 g, 1.48 mol) was added into the reaction solution dropwise over a period of 1 h. After maintaining at 0 °C for 3h, the solution was kept at room temperature for another 12 h. The reaction was monitored by TLC. After the reaction finished, the solution was washed three times by water and the organic layer was separated and collected after drying over $MgSO_4$. The organic solution was concentrated and precipitated by methanol. After filtered and washed with methanol, the final product was obtained in a 75% yield. FTIR (KBr): 1517 cm^{-1} and 1348 cm^{-1} (Ph-NO_2), 1438 cm^{-1} (P-Ph), 1231 cm^{-1} (-P=O), and 860 cm^{-1} (-C-NO_2).

Synthesis of bis(4-aminophenoxy) phenyl phosphine oxide (DAPOPPO)
DNPOPPO was placed in a round-bottom flask with 480.30g of powder tin (II) chloride dehydrate. 6000 mL ethyl acetate was introduced into the flask equipped with a condenser. The reaction mixture was stirred at room temperature for 2 h. After the solid dissolved, the solution was stirred at 60 °C for 6 h followed by cooling to the room temperature. The solution was neutralized by saturated sodium carbonate aqueous solution. The organic layer was separated and concentrated. Finally, the solution was precipitated using the petroleum ether. The obtained solid was recrystallized by CH_2Cl_2 to afford the pure product in a 90% yield. m. p. 155–156 °C. FTIR (KBr): 3448 cm^{-1} and 3345 cm^{-1} (Ph-NH_2), 1438 cm^{-1} (P-Ph), and 1256 cm^{-1} (-P=O). ^{1}H NMR (400 MHz, DMSO-d_6) δ (ppm) 7.85 (m, 2H), 7.65 (t, 1H), 7.55 (m, 2H), 6.83 (d, 4H), 6.50 (d, 4H), 5.02 (s, 4H). ^{31}P NMR (162 MHz, DMSO-d_6) δ (ppm) 11.96. ^{13}C NMR (101 MHz, DMSO-d_6) δ (ppm)

145.95, 133.10, 132.08, 131.97, 128.81, 128.67, 120.81 and 114.34. Theoretical calculation for elements of $C_{18}H_{17}N_2O_3P$ was C: 63.53 %, H: 5.04 %, N: 8.23 %, O: 14.10 %, P: 9.10 %. Found elemental contents were C: 56.89 %, H: 4.48 %, P: 7.60%.

Synthesis of polyamic acid (PAA) spinning solutions

Using the high purity diamine monomer (DAPOPPO), we had successfully synthesized a series of phosphorous-containing PAA solutions with various molar ratios of DAPOPPO/ODA. The specific example is as follows: in the reaction with a molar ratio of 1/9 (DAPOPPO/ODA), 26.20 g (0.077 mol) DAPOPPO and 138.76 g (0.693 mol) ODA were added into a flask with a stirrer, a nitrogen inlet, and a thermometer. Then 2000 mL DMAc was poured into the flask and stirred until the solid absolutely dissolved. PMDA (167.95g, 0.77 mol) was quickly added into the mixture, followed by adjusting the solid content to 15% (weight by weight) with DMAc. After overnight stirring, the isotropic solution was obtained. The other PAA solutions were prepared by the similar method, including homo-PAA and co-PAA. It was found that the viscosity of solution was too low to fabricate the fibers when the molar ratio of DAPOPPO/ODA was higher than 4/6.

Preparation of PI fibers

The PI fibers were fabricated through a two-step method. Firstly, the preparation of PAA fibers was conducted by a dry-jet wet spinning process. After filtered and degassed at room temperature, the PAA solution was extruded into the coagulation bath to form a solidifying filament followed by entering into a second washing bath. Then, the solidifying filament was dried by heating tube and collected on the winder. The PI fibers were finally obtained after thermal imidization and heat drawing.

Characterization

Fourier transform infrared (FTIR) measurement was carried out on VERTEX 70 spectrometer with the scanning wavenumber in range of 400-4000 cm^{-1} at 32 scans. Nuclear magnetic resonance (NMR) spectra were conducted on a Bruker 400 spectrometer at 400 MHz for ^{1}H NMR, 162 MHz for ^{31} P NMR and 101 MHz for ^{13} C NMR with tetramethylsilane as an internal standard. Melting points were determined on XT-4 melting point apparatus. Elemental analyses were carried out with an Elementar vario EL cube (Elementar Corporation, Germany). The inherent viscosity (η_{inh}) of PAA was measured using an Ubbelohde viscometer with a capillary inner diameter of 0.5 mm at the concentration of 0.5 dL/g (dissolve in DMAc) at 30 ^{o}C. The mechanical properties of fibers were conducted on a XQ-1 instrument with a gauge length of 20 mm and extension speed of 20 mm/min. For each group fibers, at least 10 filaments were tested and the corresponding average value was used as the final representative in accordance with GB/T 14337. The surface morphologies of the PI fibers were viewed on XL-30 scanning electron microscope (SEM) FEG (FEI Company) and the samples were sprayed with Pt before observation. Dynamic mechanical analysis (DMA) was conducted on the Rheometric scientific DMTA-V at 1 Hz along with a heating rate of 10 ^{o}C/min with the temperature ranging from 50 to 400 ^{o}C. AO exposure test was conducted in a ground-based AO effects simulation facility. The working air pressure was approximately 0.13–0.15 Pa. Discharge voltage and current were 200 V and 200 mA, respectively. PI fibers over 20 cm in length were placed on the sample tray in the vacuum chamber. Standard Kapton® films were used to calibrate exposure flux, and the final AO fluence was calculated from the mass loss of Kapton® by the following formula[30, 31].

(1)

where F is the total AO fluence (atoms/cm^2), ΔM is the mass loss of Kapton® (g), ρ is the density of Kapton® (1.42 g/cm^3), A is the exposure area of Kapton®, and E is the erosion constant of Kapton® (3×10^{-24} cm^3/atom). Table S1 presents the AO fluence adopted in current work.

3. RESULTS AND DISCUSSION

Preparation of PAA solutions and PI fibers

The inherent viscosities of PAA solutions with the diamine molar ratios of DAPOPPO/ODA varied

from 0/10 to 4/6 were listed in **TABLE 1**. As seen in **TABLE 1**, the inherent viscosity of PAA showed a decrease from 1.95 to 1.80 dl/g with increasing of DAOPPO molar content from 0% to 40%. Actually, the charge density of the amino nitrogen decreased due to the electron-withdrawing effect of phosphorous element in DAPOPPO, which caused the reactivity of nucleophilic reaction reduce. When the molar ratio of DAPOPPO/ODA was increased higher than 4/6, the viscosity of PAA solution was too low to extrude, and the fibers were unavailable.

All PI fibers were prepared from PAA fibers by thermal imidization and then the as-prepared PI fibers were drawn in heating tube to form the resulting PI fibers. The fibers were characterized by FTIR as shown in **FIGURE 1**. In the curves, the peaks at 1774 cm^{-1} and 1720 cm^{-1} corresponded to the asymmetric and symmetrica stretching vibrations of C=O group. The peak at 1360 cm^{-1} belonged to the C-N stretching vibration of imide ring, and the peak at 734 cm^{-1} was proven to the bending vibration of imide ring. The absorption bands of PAA at 1712 cm^{-1}, 1652 cm^{-1}, and 1530 cm^{-1} corresponded to the groups of C=O (COOH), C=O(CONH), and C-NH, were not found, which indicated that all the PAA fibers were successfully converted into PI fibers. Notably, the intensity of peak at 1196 cm^{-1} attributing to P=O group showed an increase with increasing of DAPOPPO content, which further indicated the successful preparation of co-PI fibers containing phosphate ester groups.

TABLE 1. Inherent viscosities of PAA solutions and mechanical properties of co-PI fibers.

Polymer No.	Diamine ratio (*m:n*)	Draft[a]/Draw[b] ratio	η_{inh} (dl/g)	Mechanical Properties		
				Tensile strength (cN/dtex)	Initial modulus (cN/dtex)	Elongation at break (%)
PI-0	0:10	2.75/1.6	1.95	5.23±0.44	79.65±3.45	11.28±0.51
PI-1	1:9	2.75/1.6	1.91	2.94±0.19	60.13±3.23	11.53±0.48
PI-2	2:8	2.75/1.6	1.86	2.58±0.24	56.01±2.65	12.60±0.49
PI-3	3:7	2.75/1.6	1.82	2.07±0.27	53.66±3.29	13.66±0.43
PI-4	4:6	2.75/1.6	1.80	1.89±0.13	51.28±2.88	14.02±0.53

[a] The ratio of the take-up speed to the extrusion speed.
[b] The ratio of after-drawing speed to before-drawing speed passing the heat tube.

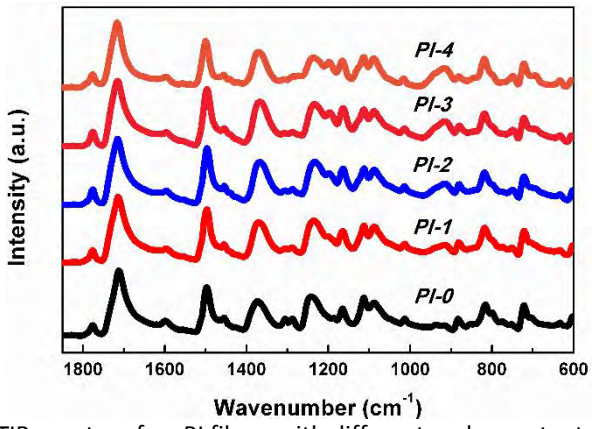

FIGURE 1. FTIR spectra of co-PI fibers with different molar content of DAPOPPO.

Thermal properties of PI fibers

The glass transition temperatures (T_gs) of the fibers were measured by DMA as depicted in **FIGURE 2**. The T_gs of PI-0, PI-1, PI-2, PI-3 and PI-4 were 400, 381, 360, 341 and 321 °C, respectively. Apparently, the incorporation of DAPOPPO caused the decrease of T_gs of the fibers, attributing that the flexibility of

molecular segment was increased with increase of ester groups in DAPOPPO.

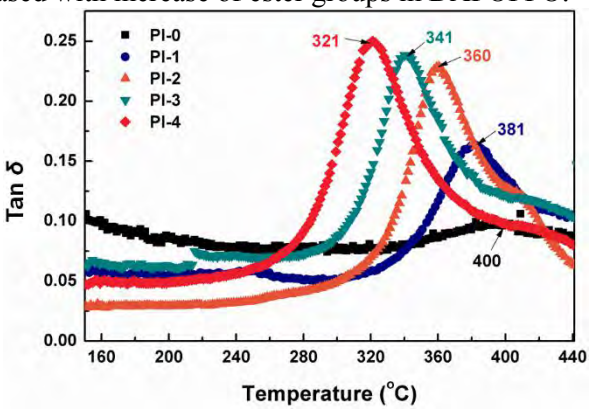

FIGURE 2. Tan δ versus temperature spectra of PI fibers with different molar content of DAPOPPO.

Mechanical properties of PI fibers

Mechanical property was an important parameter for polymeric fibers in practical applications. As shown in **TABLE 1** and **FIGURE 3**, with the increase of DAPOPPO molar content, the tensile strength and initial modulus of the co-PI fibers decreased dramatically. However, the elongation at break improved significantly. Specifically, for the pure PI fiber, the tensile strength and initial modulus showed the values of 5.23 cN/dtex and 79.65 cN/dtex, and elongation at break was 11.28%. For the PI-1, PI-2, PI-3 and PI-4, the tensile strength and initial modulus were 2.94 cN/dtex and 60.13 cN/dtex, 2.58 cN/dtex and 56.01 cN/dtex, 2.07 cN/dtex and 53.66 cN/dtex, and 1.89 cN/dtex and 51.28 cN/dtex. Notably, the elongation at break showed the values of 11.53%, 12.60%, 13.66% and 14.02%, corresponding to PI-1, PI-2, PI-3 and PI-4. Although incorporation of more DAPOPPO molar content into the PI chains led to the decrease on mechanical properties of fibers, the tensile strength and initial modulus of fibers still could satisfy the requirements for the applications of protection fields.

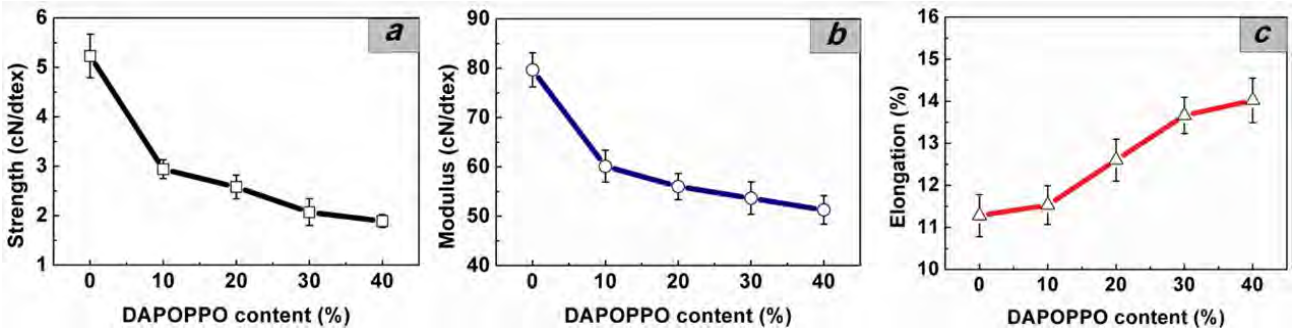

FIGURE 3. Variation of mechanical properties with DAPOPPO molar content for PI fibers.

Mass loss of PI fibers after AO erosion

The co-PI fibers were exposed to simulated AO with fluences of 6.5×10^{19} atoms cm^{-2}, 1.3×10^{20} atoms cm^{-2}, 2.3×10^{20} atoms cm^{-2} and 3.2×10^{20} atoms cm^{-2} to investigate the AO resistance performance. When the polymer materials suffered AO attack, the mass loss occurred. According to **TABLE 2**, with the AO fluences increasing from 6.5×10^{19} atoms cm^{-2} to 3.2×10^{20} atoms cm^{-2}, the mass loss of the fibers exhibited a decrease from 0.22 mg cm^{-2} to 1.52 mg cm^{-2}, from 0.16 mg cm^{-2} to 0.90 mg cm^{-2}, from 0.08 mg cm^{-2} to 0.60 mg cm^{-2}, associated to the fibers of PI-0, PI-2, and PI-4. Obviously, the mass loss of the fibers showed a decrease with the AO fluences increase. At same AO fluence, fiber with higher DAPOPPO content exhibited lower mass loss. Compared to PI-0, the fibers containing DAPOPPO showed excellent mass retention at higher AO fluence.

TABLE 2. Mass loss of PI fibers versus AO exposure with difference fluence.

Fiber No.	Diamine Ratio (m/n)	SEM Images No.	Mass loss[a] 6.5×10^{19} atoms/cm^2 (mg/cm^2)	Mass loss 1.3×10^{20} atoms/cm^2 (mg/cm^2)	Mass loss 2.2×10^{20} atoms/cm^2 (mg/cm^2)	Mass loss 3.2×10^{20} atoms/cm^2 (mg/cm^2)
PI-0	0:10	0-a ~ 0-e	0.22	0.48	1.00	1.52
PI-2	2:8	2-a ~ 2-e	0.16	0.32	0.72	0.90
PI-4	4:6	4-a ~ 4-e	0.08	0.22	0.42	0.60

[a] Using formula (1) to calculate the total AO fluence with Kapton® film.

Surface morphology and composition of the fibers after AO erosion

As seen in **FIGURE 4**, all the fibers showed smooth and uniform surface prior to AO erosion. When the fibers were exposed to the AO beam, the surfaces became rough. At lower AO fluence, surface morphologies of all PI fibers showed no clear difference. However, when the AO fluence was increased to 2.2×10^{20} atoms cm^{-2} and 3.2×10^{20} atoms cm^{-2}, PI-0 fiber showed obvious sparse, carpet-like appearance. As for the PI fibers containing DAPOPPO, the dense surface was observed, especially for PI-4 fibers. Consequently, the PI fibers with higher DAPOPPO content showed significant AO resistance even at higher AO fluence of 3.2×10^{20} atoms cm^{-2}.

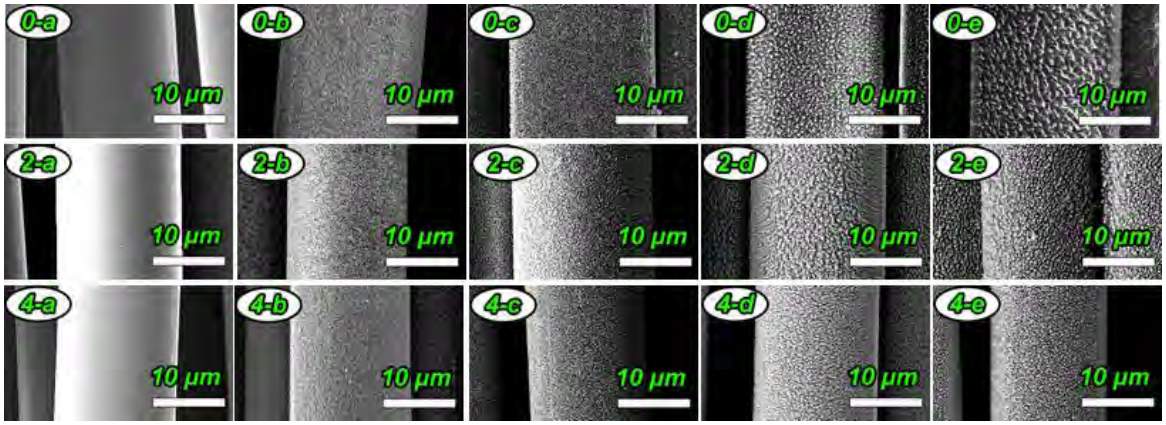

FIGURE 4. Surface morphologies of co-PI fibers after erosion by AO beam with fluence of (a) 0, (b) 6.5×10^{19} atoms/cm^2, (c) 1.3×10^{20} atoms/cm^2, (d) 2.2×10^{20} atoms/cm^2 and (e) 3.2×10^{20} atoms/cm^2.

In order to investigate the surface element composition of fibers before and after AO erosion, XPS measurements were conducted. According to **TABLE 3**, O 1s, N 1s, and C 1s peaks existed in the XPS curves of PI-0 fibers. P 2s and P 2p peaks appeared in the XPS curves of PI-2 and PI-4 fibers including O 1s, N 1s, and C 1s peaks. When the fibers were exposed to AO, concentrations of C, N and O showed no clear change. However, an obvious increase on concentration of P was observed for PI fibers containing DAPOPPO, i.e. PI-2 and PI-4. Specifically, the concentration of P showed an increase from 3.18% to 6.02%, and from 5.79% to 8.74% corresponding to PI-2 and PI-4. Moreover, the high-resolution XPS spectra of the C 1s and P 2p peaks associated to PI fibers before and after AO exposure were fitted. According to **TABLE 4**, the C 1s spectra were fitted by the C-C species at 284.8 eV binding energies (BEs), the C-N or C-O species at 287.6 eV BEs, and the C=O species at 289.0 eV BEs, which were associated to the carbon atoms of benzene rings, C-O-C in ODA or C-N-C in the imide ring, and C=O in the imide ring, respectively[32]. After AO exposure of PI-0, area of C-C species showed a decrease from 73.3% to 28.4%, whereas an increase on those of C-N or C-O species and C=O species from 9.2% to 58.9%, and 6.1% to 12.6% were observed. The similar surface composition variation of PI-4 appeared after AO exposure. The area of C-C species decreased from 40.7% to 17.67%, while area of those of C-N or C-O species and C=O species exhibited an increase from 39.9% to 67.9%, and from 19.4% to 30.2%. Notably, the area of P-(C_6H_5) at 133.3 eV BEs showed the value of 37.6% before AO exposure. However, when the fibers were exposed to AO, the P-(C_6H_5) peak disappeared, while the area of O=P at 134.6 eV BEs showed a clear increase from 62.4% to 100% (Seen in **TABLE 4**). The results indicated that C-C bond in the benzene ring of PI fibers were degraded to C-O bond, C-N bond or C=O bond

after AO exposure. Consequently, carbon elements on the surface of fibers were oxidized by AO, which released as volatiles. For the PI fibers containing PPO groups, P-(C_6H_5) band was destroyed by AO and O=P bond formed after AO erosion. Therefore, the passivated phosphate layer deposited on the fiber surface, which effectively prevented fiber from AO erosion.

TABLE 3. Surface element analysis before and after AO exposure.

SAMPLE ELEMENT	ELEMENT CONCENTRATION (atoms %)					
	PI-0		PI-2		PI-4	
PEAKS	Before AO	After AO	Before AO	After AO	Before AO	After AO
C1s	67.69	68.62	60.00	59.00	53.53	50.26
O1s	26.33	24.29	31.02	30.26	36.94	35.82
N1s	5.98	7.09	5.80	4.27	3.75	5.18
P2p	--	--	3.18	6.02	5.79	8.74

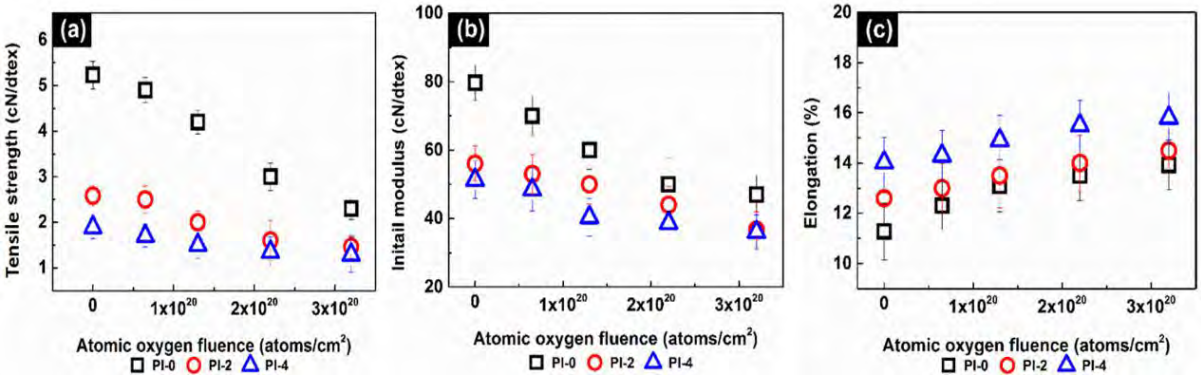

FIGURE 5. Variation of (a) tensile strength, (b) initial modulus, and (c) elongation with AO fluence.

TABLE 4. Fitted relative content for C 1s, P 2p high resolution.

ELEMENT PEAKS		Before AO exposure			After AO exposure		
		B. E.(eV)	Assignments	Area(%)	B. E.(eV)	Assignments	Area(%)
PI-0	C 1s	283.2	--	11.4	--	--	--
		284.8	C-C	73.3	284.6	C-C	28.4
		287.2	C-N, C-O	9.2	285.4	C-N, C-O	58.9
		289.0	C=O	6.1	288.5	C=O	12.6
PI-4	C 1s	284.4	C-C	40.7	284.2	C-C	17.67
		285.8	C-N, C-O	39.9	285.1	C-N, C-O	67.9
		287.8	C=O	19.4	288.2	C=O	30.2
	P 2p	133.3	P-(C_6H_5)	37.6	--	--	--
		134.6	O=P	62.4	134.1	O=P	100

Mechanical properties of the fibers after AO erosion

FIGURE 5 showed the variations on tensile strength, initial modulus, and elongation at break of co-PI fibers under different AO fluence. With AO fluence increasing from 0 atom cm^{-2} to 3.2×10^{20} atoms cm^{-2}, the tensile strengths of the PI fibers with DAPOPPO molar contents of 0%, 20%, and 40% showed decreases from 5.23 cN/dtex to 2.30 cN/dtex, 2.58 cN/dtex to 1.50 cN/dtex, and 1.89 cN/dtex to 1.29 cN/dtex, respectively. For the initial modulus of the co-PI fibers, the corresponding values declined from 79.65 cN/dtex to 47.00 cN/dtex, 56.01 cN/dtex to 37.90 cN/dtex, and 51.28 cN/dtex to 35.90 cN/dtex with increased AO fluence. Definitely, when the AO fluence was at 3.2×10^{20} atoms cm^{-2}, the retention of tensile strength and initial modulus of the fibers increased from 44% to 68% and 59% to 70% with increased DAPOPPO molar contents from 0 % to 40 wt%. Consequently, the as-prepared PI fibers containing DAPOPPO showed prominent AO resistance.

4. CONCLUSIONS

In summary, we prepared series of co-PI fibers intrinsically containing phosphorus via dry-jet wet spinning. The surface morphologies, thermal and mechanical properties, and AO resistance performance of the fibers were subsequently investigated. The results are concluded as follows:

Although the incorporation of flexible DAPOPPO chains in PI chain caused T_g decrease, good thermal properties kept for the fibers. With increasing DAPOPPO content from 0% to 40%, the mass loss of the fibers showed a significant decrease from 1.52 mg cm^{-2} to 0.60 mg cm^{-2} after AO erosion with the fluence of 3.2×10^{20} atoms cm^{-2}. SEM results indicated that PI fibers containing 40% DAPOPPO exhibited a denser surface, whereas the PI fiber without PPO group possessed a sparse carpet like surface after AO erosion. The retentions of tensile strength and initial modulus at the AO fluence of 3.20×10^{20} atoms cm^{-2} were improved dramatically from 44% to 68% and 59% to 70%, respectively. Actually, carbon elements on the surface of fibers were oxidized by AO, and the passivated phosphate layer deposited on the fiber surface after AO erosion, which effectively protected fiber from AO attack.

The excellent AO resistant performances make the co-PI fibers intrinsically containing PPO groups to be promisingly protective materials to apply in LEO.

ACKNOWLEDGEMENTS

This work has been supported by grants from the National Basic Research Program of China (973 Program, Key Project: 2014CB643604). We thank Beihang University for their help in AO experiment testing.

CORRESPONDING AUTHER

xp_q@ciac.ac.cn, zxdong@ciac.ac.cn

REFERENCES

[1]. Fischer, H.R., Tempelaars, K., Kerpershoek, A., Dingemans, T., Iqbal, M., Lonkhuyzen, H.v., Iwanowsky, B. and Semprimoschnig, C., ACS Appl. Mater. Interfaces, 2010, 2(8):2218-2225.

[2]. Minton, T.K., Wright, M.E., Tomczak, S.J., Marquez, S.A., Shen, L., Brunsvold, A.L., Cooper, R., Zhang, J., Vij, V., Guenthner, A.J. and Petteys, B.J., ACS Appl. Mater. Interfaces, 2012, 4(2):492-502.

[3]. Verker, R., Grossman, E. and Eliaz, N., Acta Mater., 2009, 57(4):1112-1119.

[4]. Liaw, D.J., Wang, K.L., Huang, Y.C., Lee, K.R., Lai, J.Y. and Ha, C.S., Prog. Polym. Sci., 2012, 37(7):907-974.

[5]. Sukhanova, T.E., Baklagina, Y.G., Kudryavtsev, V.V., Maricheva, T.A. and Lednický, F., Polymer, 1999, 40(23):6265-6276.

[6]. Cheng, Y., Dong, J., Yang, C., Wu, T., Zhao, X. and Zhang, Q., Polymer, 2017, 133:50-59.

[7]. Niu, H., Huang, M., Qi, S., Han, E., Tian, G., Wang, X. and Wu, D., Polymer, 2013, 54(6):1700-1708.

[8]. Dong, J., Yin, C., Zhao, X., Li, Y. and Zhang, Q., Polymer, 2013, 54(23):6415-6424.

[9]. Chernik, V.N., Novikov, L.S., Bondarenko, G.G., Gaidar, A.I. and Smirnova, T.N., Bull. Russ. Acad. Sci.: Phys.,

2010, 74(2):268-271.
[10]. Zhao, Y., Li, G., Dai, X., Liu, F., Dong, Z. and Qiu, X., Chin. J. Polym. Sci., 2016, 34(12):1469-1478.
[11]. Liu, F., Guo, H., Zhao, Y., Qiu, X. and Gao, L., Eur. Polym. J., 2018, 105:115-125.
[12]. Tennyson, R.C., Sur. Coat. Tech., 1994, 68-69:519-527.
[13]. Deepa, D., S., P., M., K.R. and N., N.K., J. Appl. Polym. Sci., 2004, 94(6):2368-2375.
[14]. Liu, B., Ji, M., Liu, J., Fan, L. and Yang, S., High. Perform. Polym., 2013, 25(8):907-917.
[15]. Atar, N., Grossman, E., Gouzman, I., Bolker, A., Murray, V.J., Marshall, B.C., Qian, M., Minton, T.K. and Hanein, Y., ACS Appl. Mater. Interfaces, 2015, 7(22):12047-12056.
[16]. Watson, K.A., Palmieri, F.L. and Connell, J.W., Macromolecules, 2002, 35(13):4968-4974.
[17]. Connell, J.W. and Watson, K.A., High. Perform. Polym., 2001, 13(1):23-34.
[18]. Thompson, C.M., Smith, J.G. and Connell, J.W., High. Perform. Polym., 2003, 15(2):181-195.
[19]. Connell, J.W., Smith, J.G. and Hedrick, J.L., Polymer, 1995, 36(1):13-19.
[20]. Smith, J.G., Connell, J.W. and Hergenrother, P.M., Polymer, 1994, 35(13):2834-2839.
[21]. Jeong, K.U., Kim, J.J. and Yoon, T.H., Polymer, 2001, 42(14):6019-6030.
[22]. Zhu, Y., Zhao, P., Cai, X., Meng, W. and Qing, F., Polymer, 2007, 48(11):3116-3124.
[23]. Wei, J.H., Gang, Z.X., Ming, L.Q., Rehman, S., Wei, Z.H., Dong, D.G. and Hai, C.C., Polym. Sci. Ser. B, 2014, 56(6):788-798.
[24]. Li, Z., Liu, J., Gao, Z., Yin, Z., Fan, L. and Yang, S., Eur. Polym. J., 2009, 45(4):1139-1148.
[25]. Zhao, Y., Dong, Z., Li, G., Dai, X., Liu, F., Ma, X. and Qiu, X., RSC Adv., 2017, 7(9):5437-5444.
[26]. Zhao, Y., Feng, T., Li, G., Liu, F., Dai, X., Dong, Z. and Qiu, X., RSC Adv., 2016, 6(48):42482-42494.
[27]. Zhao, Y., Li, G., Liu, F., Dai, X., Dong, Z. and Qiu, X., Chin. J. Polym. Sci., 2017, 35(3):372-385.
[28]. Liu, Y.L., Hsiue, G.H., Lee, R.H. and Chiu, Y.S., J. Appl. Polym. Sci., 1997, 63(7):895-901.
[29]. Ding, X., Qiu, X., Ma, X., Li, G., and Gao, L., Chem. J. Chinese U., 2013, 34(11):2650-2654.
[30]. Miyazaki, E., Tagawa, M., Yokota, K., Yokota, R., Kimoto, Y. and Ishizawa, J., Acta Astronaut., 2010, 66(5):922-928.
[31]. Shimamura, H. and Nakamura, T., Polym. Degrad. Stab., 2009, 94(9):1389-1396.
[32]. Duo, S.W., Li, M.S., Zhou, Y.C., Tong, J.Y. and Sun, G., J. Mater. Sci. Technol., 2003, 19(6):535-539.